Palaeontologia Electronica
http://palaeo-electronica.org

A MORPHOLOGICAL MODEL AND CT ASSESSMENT OF THE SKULL OF *PACHYRHACHIS PROBLEMATICUS* (SQUAMATA, SERPENTES), A 98 MILLION YEAR OLD SNAKE WITH LEGS FROM THE MIDDLE EAST

Michael J. Polcyn, Louis L. Jacobs, and Annat Haber

ABSTRACT

Pachyrhachis problematicus is a snake with well-developed hind limbs known from two specimens from the Cenomanian of the Middle East. One specimen has a complete and articulated, albeit crushed skull. The second specimen has a disarticulated skull crushed beneath the body. *Pachyrhachis* has recently been at the center of a debate on the origins and relationships of snakes, specifically whether *Pachyrhachis* is the sister taxon to all other snakes, or alternatively, a relatively advanced snake allied with boids and pythonids. Workers using the same specimens arrived at different interpretations of the morphology underlying the alternative hypotheses. The most complete skull was resin-embedded and acid-prepared for its original study nearly three decades ago, rendering the dorsal surface difficult to view using optical techniques, and thus significantly hampering later studies. This study utilizes CT scanning and computer reconstruction to test conflicting interpretations of morphology and thus provides a method to falsify alternative phylogenetic hypotheses. *Pachyrhachis* is found to possess an inclined quadrate with a well-developed stylohyal process and lacking a suprastapedial process, no squamosal, and a single mental foramen. The separation of exoccipitals above the foramen magnum cannot be demonstrated. There is no jugal. Confirmed morphology best supports the phylogenetic hypothesis that *Pachyrhachis* is a basal macrostomatan snake. Limb retention in a basal macrostomatan snake implies that loss of hind limbs occurred multiple times within Serpentes.

Michael J. Polcyn. Department of Geological Sciences, Southern Methodist University, Dallas, Texas 75275, USA mpolcyn@mail.smu.edu
Louis L. Jacobs. Department of Geological Sciences, Southern Methodist University, Dallas, Texas 75275, USA jacobs@mail.smu.edu
Annat Haber. Department of Geological Sciences, Southern Methodist University, Dallas, Texas 75275, USA h_annat@yahoo.com

KEY WORDS: Cretaceous; *Haasiophis*; Israel; Macrostomata; Taphonomy

Polcyn, Michael J., Jacobs, Louis L., and Haber, Annat, 2005. A Morphological Model and CT Assessment of the Skull of *Pachyrhachis Problematicus* (Squamata, Serpentes), A 98 Million Year Old Snake with Legs from the Middle East, *Palaeontologia Electronica* Vol. 8, Issue 1; 26A:24p, 2.9MB; http://palaeo-electronica.org/paleo/2005_1/polcyn26/issue1_05.htm

PE Article Number: 8.1.26

Submission: 13 October 2004. Acceptance: 7 April 2005

INTRODUCTION

The Cenomanian snake, *Pachyrhachis problematicus*, is known from two specimens from limestone quarries near 'Ein Yabrud, in the West Bank, north of Jerusalem. One specimen has a complete and articulated, albeit crushed, skull (Haas 1979, 1980a). In the second specimen, a disarticulated skull is crushed below the ribcage (Haas 1980b). Phylogenetic analysis by Caldwell and Lee (1997) places *Pachyrhachis* as the basal member or sister taxon of Serpentes. However, that phylogenetic hypothesis was tested and falsified by Zaher (1998), who concluded that *Pachyrhachis* was instead a basal macrostomatan allied with boids and pythonids. Disagreement regarding the phylogenetic position of *Pachyrhachis* persisted (Lee and Caldwell 1998; Caldwell 1999, 2000; Zaher and Rieppel 1999b, 2000; Rieppel and Zaher 2000a, 2000b), culminating in a seemingly intractable impasse (Rieppel and Kearney 2001). On the basis of a data set developed independently, Tchernov et al. (2000) found *Pachyrhachis* and a second taxon from 'Ein Yabrud, *Haasiophis,* to be basal macrostomatans (see also Rieppel et al. 2003; Zaher and Rieppel 2002; Lee and Scanlon 2002a, 2002b). The same specimens and general observational techniques used by all workers led to conflicting interpretations of morphology. Cladistic analyses based on those interpretations subsequently yielded different phylogenetic hypotheses.

The source of differing interpretations of morphology derives from HUJ [The Hebrew University of Jerusalem]-PAL 3659. This specimen is difficult to study due to a number of taphonomic factors, further complicated by preparation techniques. George Haas (1979) of the Hebrew University of Jerusalem originally described *Pachyrhachis* using only HUJ-PAL 3659, which includes the crushed but beautifully articulated skull originally preserved on a limestone flag. After describing the dorsal surface of the skull (Haas 1979; see also Haas 1980a, 1980b), the specimen was embedded in resin and the ventral surface was acid prepared and described (Haas 1980a). Subsequent to Haas's original description, the dorsal surface could only be viewed through the embedding resin. Additionally, the resin was covered with glass, which at some point was broken, further obscuring the view. The glass has since been removed, but the resin remains. The viability of optical techniques for examination of the morphology of HUJ-PAL 3659 is compromised due to taphonomic factors including crushing, breakage, overlapping elements, displacement during preservation, matrix residue from mechanical preparation on the dorsal surface of the skull, and to subsequent resin embedding of the dorsal surface for acid preparation of the ventral surface (Figure 1).

Figure 2 shows three renderings of the dorsal surface of the articulated skull of *Pachyrhachis* as

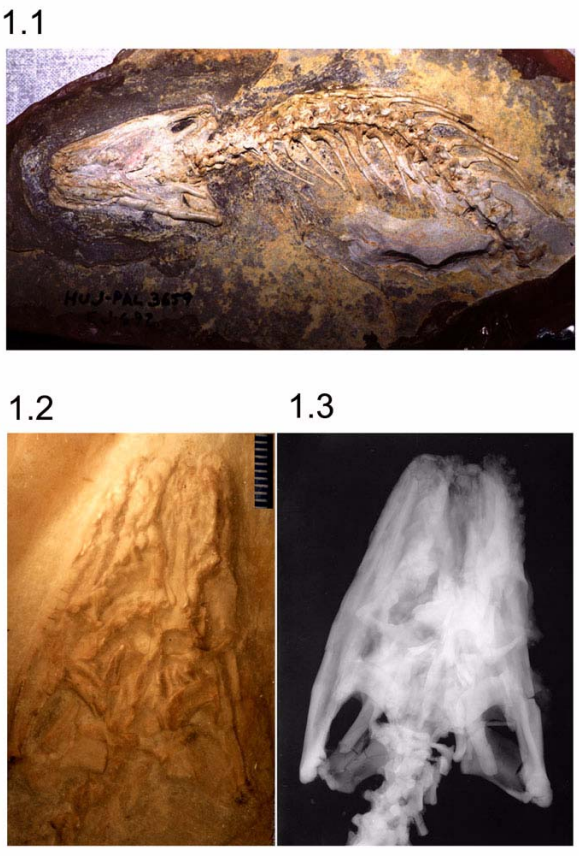

Figure 1. *Pachyrhachis problematicus* (HUJ-PAL 3659) images demonstrating the state of preservation and conservation at the time of restudy by Caldwell and Lee (1997) and Rieppel and Zaher (1999b). 1.1, resin plaque exposing ventral view of specimen. approximately 18 cm long. 1.2, dorsal surface of the skull viewed through resin. scale in millimeters. 1.3, radiograph employed by Rieppel and Zaher (1999b), scale as in 1.2.

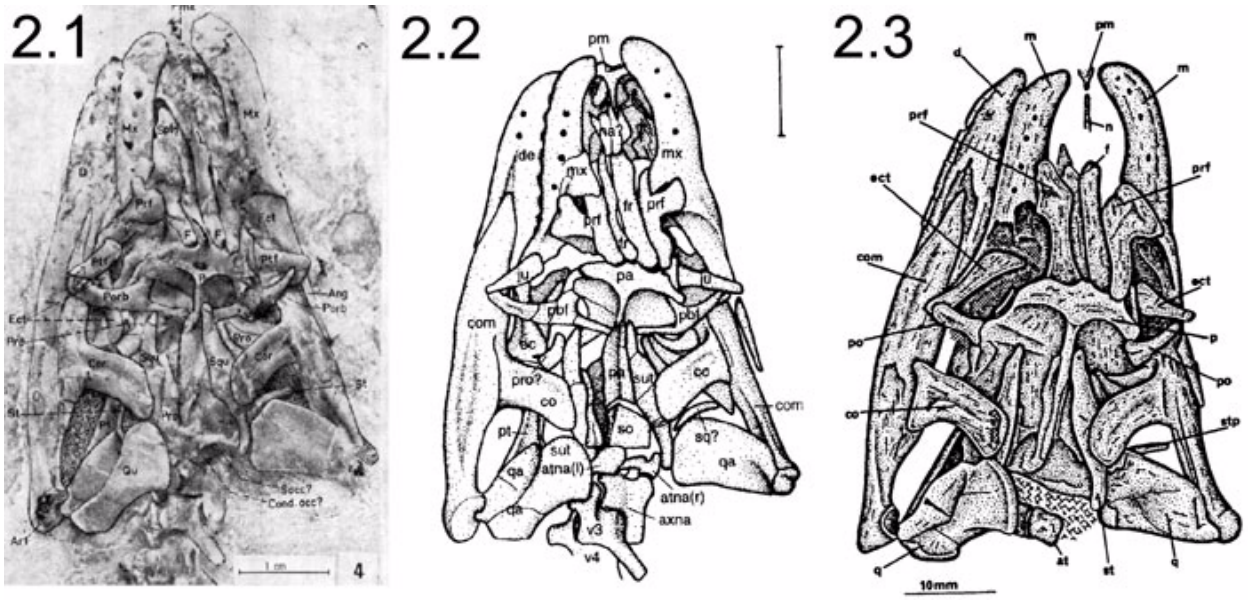

Figure 2. Interpretive drawings of the dorsal skull surface of *Pachyrhachis problematicus* (HUJ-PAL 3659) illustrating conflicts in interpretation of morphology. 2.1**,** Haas (1979, figure 3). 2.2**,** Caldwell and Lee(1997, figure 1a). 2.3, Rieppel and Zaher (1999b, figure 1). Abbreviations used in figures: Haas, 1979 (ang, angular; atna, atlas neural arch; axna, axis neural arch; com, compound bone; co, coronoid; d, dentary; ect, ectopterygoid; f, frontal; mx, maxilla; p, parietal; pmx, premaxilla; porb, postorbital; prf, prefrontal; ptf, postfrontal; pro, prootic; squ, squamosal; qu, quadrate; socc, supraoccipital; spt, septomaxilla; porb, postorbital; squ, squamosal; st, stapes); Caldwell and Lee 1997 (pm, premaxilla; mx, maxilla; de, dentary; prf, prefrontal; fr, frontal; ju, jugal; pof, postorbitofrontal; pa, parietal; com, compound bone; ec, ectopterygoid; co, coronoid; pro, prootic; sq, squamosal; qa, quadrate; so, supraoccipital; pt, pterygoid; atna, atlas neural arch; axna, axis neural arch; sq, squamosal); Rieppel and Zaher, 1999b (at, atlas neural arch; axna, axis neural arch; com, compound bone; co, coronoid; d, dentary; ect, ectopterygoid; f, frontal; mx, maxilla; n, nasal; p, parietal; pm, premaxilla; po, postorbital; prf, prefrontal; q, quadrate; spt, septomaxilla; porb, postorbital; squ, squamosal; st, supratemporal; stp, stapes).

taken from Haas (1979), Caldwell and Lee (1997), and Zaher and Rieppel (1999b). Given the complexity and history of HUJ-PAL 3659, it is not surprising that there are some differences in the interpretations as illustrated in Figure 2, differences that contributed to varying phylogenetic placement of *Pachyrhachis.* Although Haas recognized a number of diagnostic snake characters, he considered *Pachyrhachis* a highly derived platynotan or varanoid lizard. Caldwell and Lee (1997) recognized *Pachyrhachis* as a snake and the sister taxon to all other snakes, and that clade as the sister taxon to mosasauroids, resurrecting Cope's (1869) concept of Pythonomorpha (see also Lee 1997a, 1997b, 1998; Lee and Caldwell 1998; Caldwell 2000). Zaher (1998) reinterpreted *Pachyrhachis* as an advanced snake, specifically a basal macrostomatan allied with boas and pythons (see also Zaher and Rieppel 1999a; Rieppel and Zaher 2000a, 2000b).

Snakes such as *Pachyrhachis, Haasiophis*, and *Eupodophis,* which possess all the bony elements of the hind limb (as opposed to the rudimentary limb and girdle elements of modern worm snakes, boas, and pythons), are primitive in that attribute. However, the issue of macrostomatan versus more primitive phylogenetic placement hinges in large part on conflicting morphological interpretations of skull elements (Rage and Escuillié 2000; Tchernov et al. 2000; Rieppel et al. 2003). The major differences among the three interpretations that are important here are: 1) the morphology and orientation of the quadrate; 2) the identification of the stapes or squamosal; 3) the number of mental foramina; 4) the identity of the bones in the circumorbital series; 5) the question of whether the exoccipitals contact above the foramen magnum; and 6) presence of a dorsal prefrontal process of the maxilla.

To test conflicting interpretations of morphology, the articulated skull of *Pachyrhachis* (HUJ-PAL 3659) was scanned using X-ray computed tomography (CT). Two- and three-dimensional reconstructions were computer generated to expose details from viewing perspectives that could not be attained using optical techniques. We also created a three-dimensional digital model of the skull utilizing specific measurements as bound-

aries. By removing distortion due to crushing, we were able to test the feasibility of the identification of the most problematic bones of the circumorbital series, the ectopterygoid, and the orientation and morphology of the quadrate. This model then provides a hypothesis of the appearance of the undistorted skull of *Pachyrhachis*. The value of digitally modeling morphology in this case is in providing a more precise identification of structures. It is fundamentally a taphonomic exercise to remove compaction, rotation, and distortion.

Agreement among investigators on primary observations of morphology is critical to the phylogenetic understanding of snakes with hind limbs. A morphological feature either exists, does not exist, or it remains ambiguous or unknown. We intend to elucidate and clarify what can or cannot be seen in the fossil using optical observation and CT derived digital data and provide the basis from which competing phylogenetic hypotheses can be tested and falsified. An independent phylogenetic analysis is beyond the scope of this study, which is intended only to test the data quality of previous primary observations and to discover new data.

MATERIALS AND METHODS

CT Scanning

The resin embedded skull (HUJ-PAL 3659) presents the ventral surface exposed on an epoxy resin plaque, retaining traces of the original limestone matrix on the surface. The epoxy resin holding the specimen is approximately 17.5 mm thick, 75 mm wide, and 195 mm long. The skull was scanned at the University of Texas at Austin High-Resolution CT Facility (tube voltage 150 kV, 0.16 mA, no filter, air wedge, 190% offset, slice thickness of 0.24 mm, S.O.D. of 130.0 mm, 1800 views, 1 sample per view, interslice spacing of' 0.2 mm, field of reconstruction is 70.0 mm, reconstruction offset 600, reconstruction scale 75). This resulted in 308 transverse slices at ~137 micron interpixel resolution and a slice thickness of 240 microns; each slice was saved as a 512 X 512 pixel tiff image in both 16 bit and 8 bit modes (Appendix 1). The sequential 308 slices together form a three-dimensional matrix, and each pixel representing a volume element (voxel) in a three-dimensional framework. Variations in the value of each voxel represent variations in relative X-ray attenuation, which closely mirror compositional variations. X signifies the transverse axis, Y the dorsoventral axis, and Z the longitudinal axis of the CT data set. Voxblast version 3.0 (VayTek 2000) was used to build rendered and lighted isosurface and sectional reconstructions. Voxblast was also used to resample the original 308 slice stack in the XZ plane, in order to isolate the 93 slices that contain the specimen–thus reducing the file size and memory requirements for processing, and providing better sectional illustrations for comparison with isosurface reconstructions. ImageJ version 1.32i (Rasband 2003) was used for analysis and tracing of slices and Adobe Photoshop 6.0 (Adobe Systems, Inc. 2001) for cropping and rotation of the original data set as well as increasing voxel density using the bicubic method of resampling. The latter process was used to optimize the isosurface reconstruction abilities of Voxblast, providing a more voxel-dense volume, thereby minimizing aliasing effects.

CT scanning and computer reconstruction have resolving limitations. These are manifested in spatial resolution, X-ray attenuation differentiation, noise artifacts, and reconstruction artifacts. Specimen geometry greatly influences both the available spatial resolution and artifacts caused by variation in X-ray scatter and differential absorption due to the amount and composition of material intersected by the X-rays at different angular rotations. Ideal specimens are cylindrical and small enough to sit close to the X-ray source, providing magnification via the fan beam projection onto the X-ray detectors. In the case of HUJ-PAL 3659, specimen size and geometry were less than optimal, presenting a long rectangular cross section, with the area of interest small relative to the block size, thereby reducing beneficial magnification. Serial sections do not clearly delineate individual elements but show centers of greater attenuation, allowing elements to be traced through the volume. Additionally, software problems encountered during the scanning process forced multiple interruptions and restarts, resulting in slice misalignment in the anterior and midsection of the skull and vertebral column. These misalignments are visible in the isosurface reconstructions as transversely oriented lines on the anterior portion of the skull and vertebral column. A loss of data in the midsection of the skull occurred during one of the scan interruptions, constituting approximately five slices and amounting to about a 1 mm gap, and is represented by the thick black transversely oriented line across the midsection of the skull in the CT reconstructions (Figure 3; see also Appendix 2). The methods employed here are not perfect; however, they provide an independent test of previous optical and X-radiograph observations and augment our knowledge of the morphology of this specimen. Comparison with light photographs demonstrates the superiority of CT techniques in eliminating lighting artifacts such as shadow and specularity, and pro-

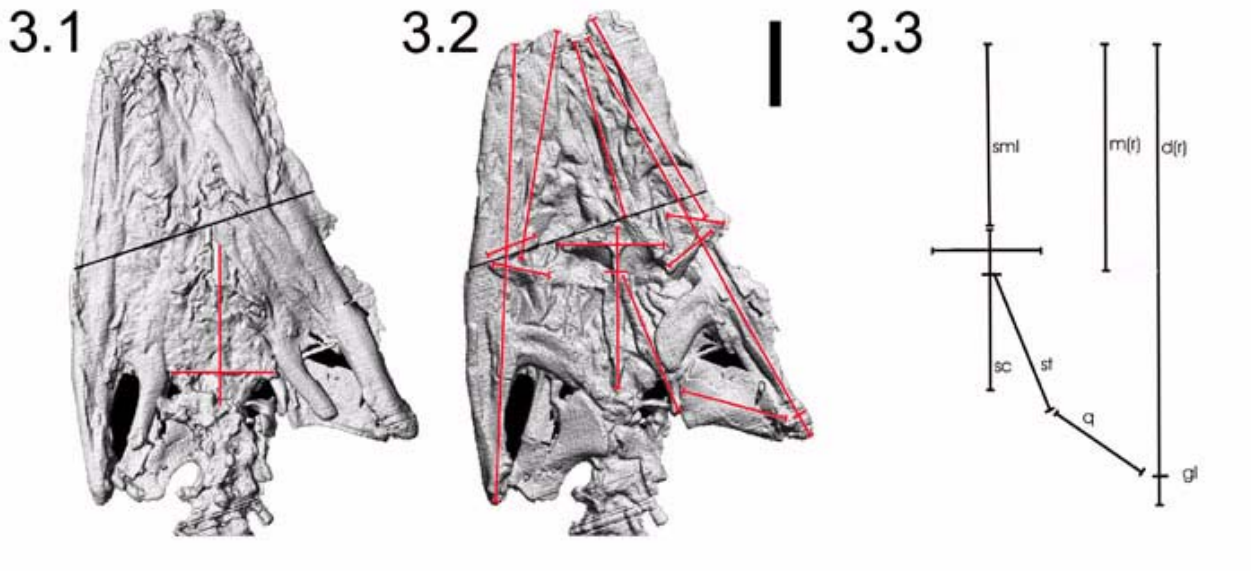

Figure 3. Three-dimensional isosurface models derived from CT data and line segment stand-ins to test alignment and displacement of cranial elements of *Pachyrhachis problematicus* (HUJ-PAL 3659). 3.1, Ventral view with lines indicating sagittal plane traced from the median basioccipital to the parasphenoid rostrum and transverse planes indicating lateral limits of exoccipitals. 3.2, Dorsal view with lines indicating sagittal and transverse planes traced on parietal, and line segments to act as stand-ins for major elements and landmarks. 3.3, Line segment stand-ins, rotated and adjusted to remove translational and rotational distortion of major elements. Abbreviations: d, dentary; gl, glenoid; m, maxilla; pob, postorbital; q, quadrate; sc, sagittal crest; sml, sagittal mid-line; st, supratemporal. Scale bar equals one centimeter.

vides a clearer illustration of topology and true morphology (Appendix 2). Additionally, the protocols outlined retain digital data representing a facsimile of the specimen, and therefore a testable data set (Appendix 1). Moreover the methods described herein can be duplicated and improved upon if so desired and therefore presents a superior level of testability and reproduction of results compared tooptical examination or X-radiographs alone.

Taphonomic Distortion

Figures 3.1 and 3.2 display isosurface images of the dorsal and ventral surfaces of the skull of *Pachyrhachis*. The ventral surface is reversed so landmarks can be stacked in order to recognize and remove distortion (Figure 3.1, see also Appendix 3). A line from the center of the basioccipital through the parasphenoid rostrum defines the midline of the skull (Figure 3.1). The posterior midline of the dorsal surface indicated by the sagittal crest lies above the ventral midline (Figure 3.2). As the skull was crushed, the snout rotated to the left, with the right maxilla overlying the tip of the right dentary and the left dentary displaced laterally but lying on its medial surface. The skull of *Pachyrhachis* is crushed dorsoventrally, with individual elements suffering varying degrees of compaction and displacement. The left and right postorbitals are symmetrically displaced laterally, and the coronoid processes of the lower jaws are collapsed medially on both sides. The symmetry of structures and their crushing patterns across the skull are important because they indicate force applied orthogonal to the bedding plane on which the specimen was preserved.

To quantify the amount of displacement of each element, the ventral isosurface reconstruction was rotated 18.4 degrees relative to the original scanning axis to approximate the alignment of the center of the parasphenoid and the posterior center of the basioccipital (Figure 3.1) at a reference angle of 0.0 degrees. The dorsal isosurface was then rotated -18.4 degrees to match the alignment of the ventral surface. By comparing the dorsal sagittal alignment of the parietal to that of the basioccipital-basisphenoid, it is clear that the braincase behaved as a single unit with respect to crushing (Figure 3.2; see also Appendix 3).

The parietal-basicranium midline was used as a reference of 0.0 degrees. In dorsal view the posterior terminus of the medial suture of the frontals is displaced slightly right of center, the suture angles 15.5 degrees to the left anteriorly. The prefrontals approximate this displacement to an equivalent degree. The right maxilla is preserved in a slightly more anterior position than the left. The small edentulous premaxilla is preserved in place between the anterior maxillaries. The right mandi-

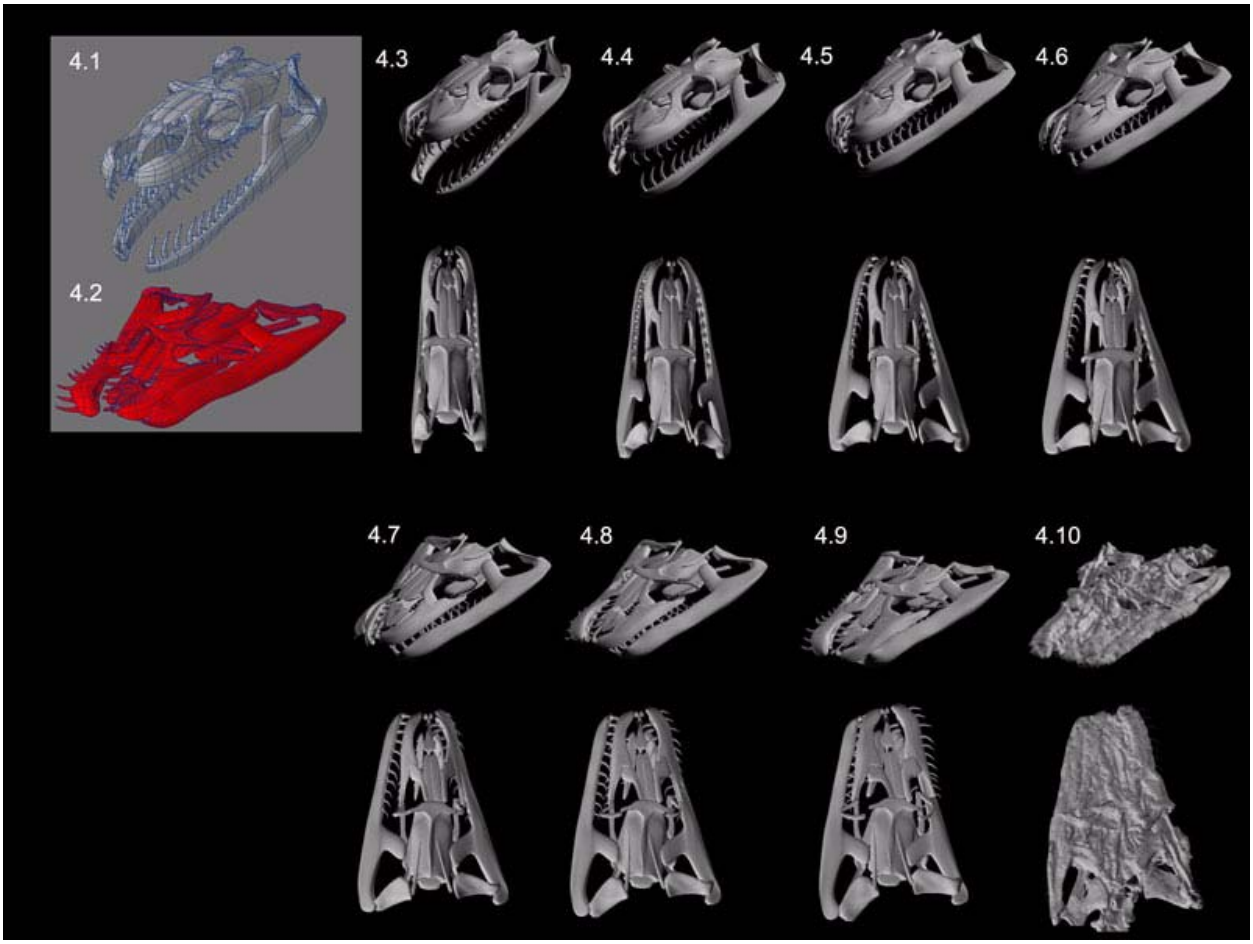

Figure 4. Morphological model of *Pachyrhachis problematicus* simulating effects of crushing: (4.1) Uncrushed state, and (4.2) crushed state. 4.3-4.9, oblique (top) and dorsal (bottom) views of taphonomic simulation: 4.3, uncrushed state; 4.4, initial collapse of dentaries and quadrates; 4.5-4.9, progressive crushing and leftward rotation of snout relative to the braincase due to right dentary underlying right portion of snout, counterclockwise rotation of quadrates, dorsal portion of postorbitals displaced laterally, and the ventral portion of postorbitals following the position of the anterior ectopterygoids; 4.10, isosurface model of current crushed state based on CT data (of HUJ-PAL 3659) for comparison to crushed simulation. Note final resting position of ventral portion of postorbital relative to anterior ectopterygoids; see also Appendix 4 for animation of crushing sequence. The degree of gape in the uncrushed state is subjective; however, the position of anterior tips of dentaries as preserved indicate their relatively close proximity anteriorly and the relationship of the mandibles to the quadrate constrains them posteriorly, suggesting the mandibles were more or less in life position as the carcass came to rest.

ble is in articulation with the distal quadrate and displaced anteriorly to the left 29.0 degrees, underlying the skull and invading the natural position of the right ectopterygoid. The left mandible is preserved adjacent to the left side of the skull, embracing the left maxilla.

All relative displacement of elements including the snout, frontals, prefrontals, the left mandible, the left supratemporal, and the sagittal crest is leftward. All rotation of elements is counterclockwise, including the quadrates, with the left displaced medially and slightly overlapping the anterior vertebral column.

Morphological Model

The morphological model (Figure 4.1) was constructed by building polygon surfaced wireframe simulation elements using Lightwave 3D, version 8 (Newtek 2004) and employing the three-dimensional isosurface model derived from the CT data as a guide. Removal of distortion from the elements was somewhat subjective; however, care was taken to approximate surface areas and lengths of the CT model in the proxy models of individual elements. The proxy elements were then manipulated to determine best fit to one another. Finally, the elements were distorted to mimic the distortion present in the CT data representing the actual fossil by manipulating the models (Figure

4.2). The undistorted and distorted reconstructions were then used as end points in a time sequence animation to simulate the interaction of elements and the relative timing and effects of crushing (Figure 4.3-4.9; see also Appendix 4 for animation sequence).

Institutional Abbreviations

HUJ, Hebrew University of Jerusalem; UCMP, University of California Museum of Paleontology; TMM, Texas Memorial Museum, Austin Texas; CAS, California Academy of Science.

Specimens Examined

Pachyrhachis problematicus HUJ-PAL 3659; *Cylindrophis ruffus* CAS 231481; *Cylindrophis ruffus* UCMP 136995; *Anilius scytale* TMM(VPL) M-8281; *Xenopeltis unicolor* TMM(VPL) M-8276; *Xenopeltis unicolor* TMM(VPL) M-8277; *Python regius* TMM(VPL) M-8278; *Python curtis* TMM(VPL)M-8279; *Epicrates cenchria* TMM (VPL) M-8280.

RESULTS

The computed tomography and computer generated three-dimensional isosurface reconstruction techniques employed here yield results comparable to high fidelity casts enabling viewing of morphology in three axes of rotation. Additionally, serial sections illustrate topological relationships of individual elements, providing better understanding of those that are obscured by overlapping elements or matrix residue. Figure 5.1 is a low angle light photograph of the ventral surface of the specimen as preserved today. Figure 5.2 is the same view using the isosurface reconstruction of the CT data set. Comparison of Figures 5.1 and 5.2 demonstrates the fidelity and therefore the viability of computer generated reconstruction of CT data for illustrative and quantitative purposes and provides a qualitative reference for subsequent discussion of the resin obscured dorsal surface of the skull. The isosurface reconstruction of the resin embedded dorsal surface is represented in Figure 5.4 as a stereo pair. Figures 5.3 and 5.5 are interpretive line drawings derived from isosurface reconstructions, photographs, and microscopic study of the specimen. Elements that have been the subject of conflicting interpretation are indicated by ue1 through ue5 (unidentified elements) and are referenced in the following sections.

Orientation and Morphology of the Quadrates

The relationship of the quadrate to the supratemporal dorsally and the glenoid of the compound bone of the lower jaw ventrally is largely preserved on the right side, but the quadrate is rotated counterclockwise (Figures 3, 6). Caldwell and Lee (1997) reconstructed *Pachyrhachis* with vertically oriented quadrates with broad lateral facing surfaces. To test this reconstruction, the length, orientation, and position of morphological landmarks were traced on the dorsal surface of the skull, including the maximum length of the mandibles as well as the center of the glenoid, maxillae, parietal-supraoccipital midline, snout midline, right supratemporal, and right quadrate (Figure 3.2). These tracings were then rotated and adjusted to parallel one another and align the anterior terminus of the premaxillae, maxillae, and mandibles (Figure 3.3).

The position of the right supratemporal was retained and taken to approximate the natural position for three reasons: 1) the primary force that crushed the specimen was orthogonal to the bedding plane as previously discussed; 2) this primary force also manifested in the leftward displacement of the left supratemporal and the leftward crushing of the sagittal crest (as the result of a leftward incline of the skull due to the right mandible underpinning the right side of the skull, which influenced left lateral but not anterior displacement); and 3) asymmetrical rotation and outward collapse of the quadrates was not likely to have contributed to anterior displacement as evidenced by the fact that the quadrates were crushed laterally, not dorsoventrally. This would most likely be the case if the quadrates splayed out prior to the remaining portion of the skull being crushed, and thus the resistive forces of the quadrates would be more medially oriented, not anteriorly.

The supratemporals in *Pachyrhachis* are long relative to other snakes. As preserved, the posterior free-ending extensions of the supratemporal comprise approximately one-third their total length. The anterior ends reach anterior to the anterior terminus of the prootic. In Recent snakes the supratemporal does not extend anterior to the anterior terminus of the prootic, and in that respect may justify a more posterior reconstruction. However, reconstruction of the supratemporals in a more posterior position would in fact exaggerate the macrostomatan condition of the distal extension of the supratemporal beyond the skull roof. The supratemporal and the parietal are developmentally part of the dermatocranium whereas the prootic is a part of the chondocranium and thus do not share obvious developmental relationships that would preclude the supratemporal anterior terminus exceeding that of the prootic. Given the taphonomic affects discussed and in absence of developmental constraints, the proportionality of sutured versus free-end of the supratemporal and

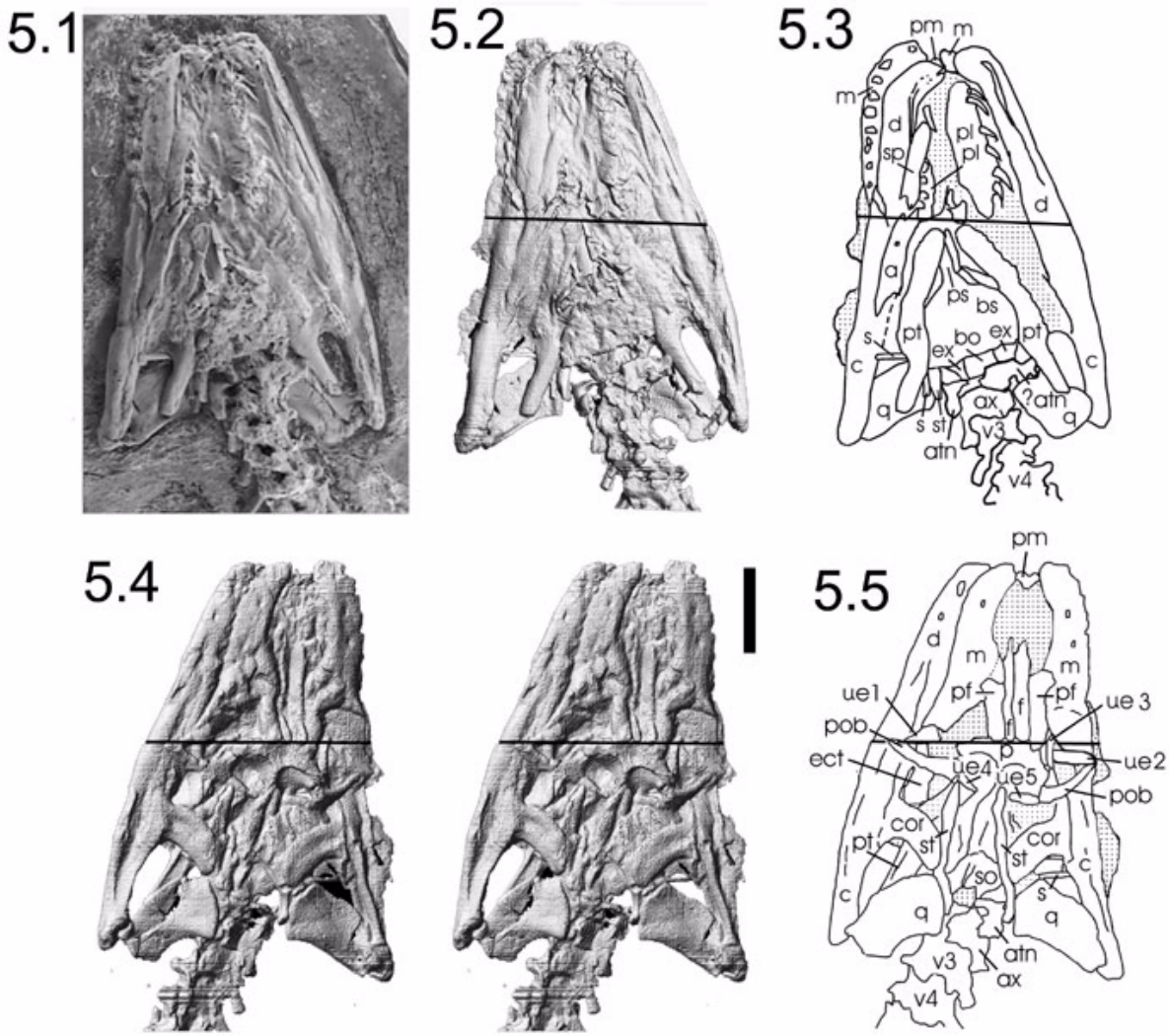

Figure 5. Photograph and computer reconstructions derived from CT data, and interpretive line drawings of *Pachyrhachis problematicus* **(**HUJ-PAL 3659). 5.1, light photograph of ventral surface as currently conserved; 5.2, computer reconstructed isosurface model derived from CT data. Note resolution and fidelity of surface reconstruction as compared with light photograph. 5.3, interpretive drawing of ventral surface; 5.4, stereopair of dorsal surface from computer reconstructed surface model derived from CT data; 5.5, interpretive drawing of dorsal surface. Abbreviations: a, angular; atn, atlas neural arch; ax, axis vertebra; bs, basisphenoid; bo, basioccipital; c, compound bone; cor, coronoid; d, dentary; ect, ectopterygoid; ex, exoccipital; f, frontal; m, maxilla; p, parietal; pm, premaxilla; pob, postorbital; pf, prefrontal; pl, palatine; pt, pterygoid; q, quadrate; s, stapes; so, supraoccipital; sp, splenial; st, supratemporal, ue1-5; unidentified elements; v3-v4, 3rd and 4th cervical vertebra. (See also Appendices 2, 3.) Scale bar equals one centimeter.

the position of the anterior terminus relative to the anterior extent of the prootic is deemed reasonable.

Taking the length of the quadrate along its midline, the right quadrate requires 19 degrees of inclination to achieve articulation with both the mandibular glenoid posteroventrally and the supratemporal anterodorsally. The degree of inclination is of course controlled by both the position of the supratemporal and the position of the mandible. Therefore, the mandibular articulation surface of the quadrate was examined and compared with a number of alethinophidian and macrostomatan snakes to determine if the trochanter morphology could be used to determine orientation of the articulation. In specimens examined that possess a vertical or nearly vertical quadrate (e.g., *Cylindrophis ruffus, Anilius scytale, Xenopeltis unicolor,*

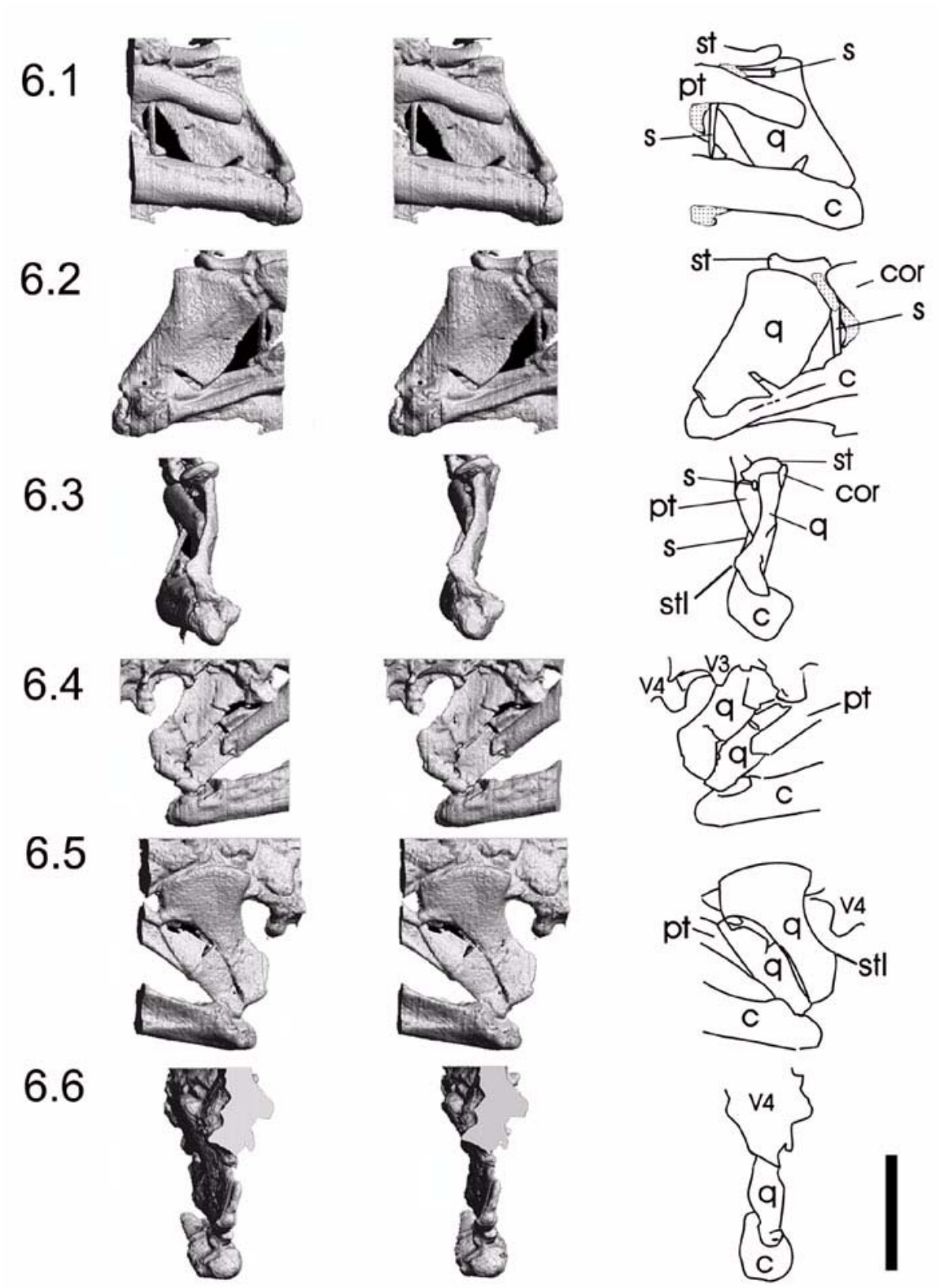

Figure 6. Stereopairs of quadrates of HUJ-PAL 3659, from computer reconstructed isosurface model derived from CT data and associated interpretive line drawings: 6.1-6.3**,** right quadrate in (6.1) medial, (6.2) lateral, and (6.3) posterior view; 6.4-6.6, left quadrate in (6.4) medial, (6.5) lateral, and (6.6) posterior view. Abbreviations: c, compound bone; cor, coronoid; pt, pterygoid; q, quadrate; s, stapes; st, supratemporal; stl, stylohyal process; V3-V4, 3rd and 4th cervical vertebra. (See also Appendix 5 for animated reconstruction sequence.)

Python regius), the trochanter was symmetrical in lateral view. In specimens possessing a slightly posteroventrally inclined quadrate (e.g, *Epicrates cenchria*) the trochanter was asymmetrical with the majority of the trochanter restricted to the anterior portion. In *Pachyrhachis,* the trochanter is obscured on the right quadrate, but a well-defined trochanter is present on the anteroventral surface of the left quadrate (Figure 6.4), but not on the posteroventral surface (Figure 6.5). Thus, the articulating surface was predominantly restricted to the anterior portion of the distal quadrate, and therefore, the quadrate was not vertical in *Pachyrhachis*, but inclined to a moderate degree. This condition is consistent with the position and length of the supratemporal.

The quadrates in *Pachyrhachis* are preserved with a broad lateral profile due to crushing. The crushed state of the quadrate was apparently interpreted by Caldwell and Lee (1997) as the true morphology as addressed in their description and reconstruction. We disagree with this interpretation. During crushing, the distal portion of the quadrates was rotated relative to the cephalic condyles yielding the broad surface as preserved. In snakes the quadrate articulation with the supratemporal where present is in para-sagittal plane and the mandibular condyle long axis is oriented orthogonal to the mandibular axis. Removal of distortion introduced by crushing was achieved by aligning the cephalic condyle with the sagittal plane and rotating the mandibular condyle to bring it roughly orthogonal to the sagittal plane, distributing the rotation linearly along the length of the quadrate (see Appendix 5 for details of reconstruction).

Stapes

The elements that Haas (1979) referred to as squamosals are the supratemporals as recognized by later authors. The tentative squamosal of Caldwell and Lee (1997) is the proximal portion of the right stapes as identified by Zaher and Rieppel (2002). The distal end of the stapes was correctly identified by Caldwell and Lee (1997) but incorrectly identified as the opisthotic paroccipital process by Zaher and Rieppel (2002). The element in question is sandwiched between the posterior pterygoid quadrate ramus, the distal supratemporal, and the quadrate (Figure 6.1-6.3). Apparently, the right stapes is broken or bent along its shaft. Our identification of this element as the stapes is supported by tracing it in serial sections 180 to 240 and 280 to 305 (Figure 7). The shafts representing both the proximal and distal portions of the right stapes are visible in the same plane. The stylohyal process of the quadrate is visible in Figure 6.3, 6.6. The reconstructed length of the stapes is consistent with the distance from the stylohyal process to the inferred position of the fenestra ovalis (Figure 4).

Comments. The supratemporal is extremely reduced or absent in scolecophidians (Zaher and Rieppell 2002) and the quadrate abuts the sidewall of the braincase. In alethinophidians examined (e.g., *Cylindrophis ruffus, Anilius scytale)*, the supratemporal is relatively short and the quadrate is supported by both the supratemporal and the braincase and the stapes articulates with a posteriorly directed suprastapedial process of the quadrate via a separate intervening calcified cartilage (extracolumella or stylohyal) as is the case in *Dinilysia* (Rieppell 1979, figure 4 A, B; see also Caldwell and Albino 2002 for discussion of *Dinilysia*). In macrostomatans examined (e.g., *Python regius*, *Python curtis, Epicrates cenchria)*, the supratemporals project posteriorly and provide sole support of the quadrate (see also Rieppell 1979, figure 4C), and the stapes articulates with the middle to distal medial quadrate shaft via a fused calcified cartilage, the stylohyal. In all macrostomatan specimens examined the quadrate shaft exhibits a medial protuberance at the point of articulation with the stapes, the stylohyal process. *Pachyrhachis* is found to lack a suprastapedial process and is shown to possess a stylohyal process on the distal medial quadrate shaft (Figure 6.3). Thus, evidence provided by the free-ending supratemporal, presence of a stylohyal process, correction of the orientation of the cephalic and distal condyles and resulting morphology of the quadrate, and the posteroventral inclination of the quadrate from the supratemporal to the articular agree best with the condition in macrostomatan snakes (see Appendix 5 for reconstruction of quadrate).

Number of Mental Foramina

A single mental foramen is visible in both isosurface and sectional views. The second foramen illustrated by Caldwell and Lee (1997, figure 1A; see also Figure 2.2 this paper) is an artifact of crushing into the void formed by the Meckel's groove anterior to the anterior terminus of the surangular (Figure 8.1, 8.4-8.7, arrow 3; see also Appendix 2). Tracing through the slices, it is apparent the depression opens into the Meckel's groove. Also, a third depression on the antrolateral surface of the left dentary superficially resembles a foramen (Figure 8.1, arrow 1). However, this structure lies within a crushed and distorted area and is merely an artifact of preservation. In life, the anterior tips of the dentaries curved sharply medially, approximating the dorsal outline of the maxillae.

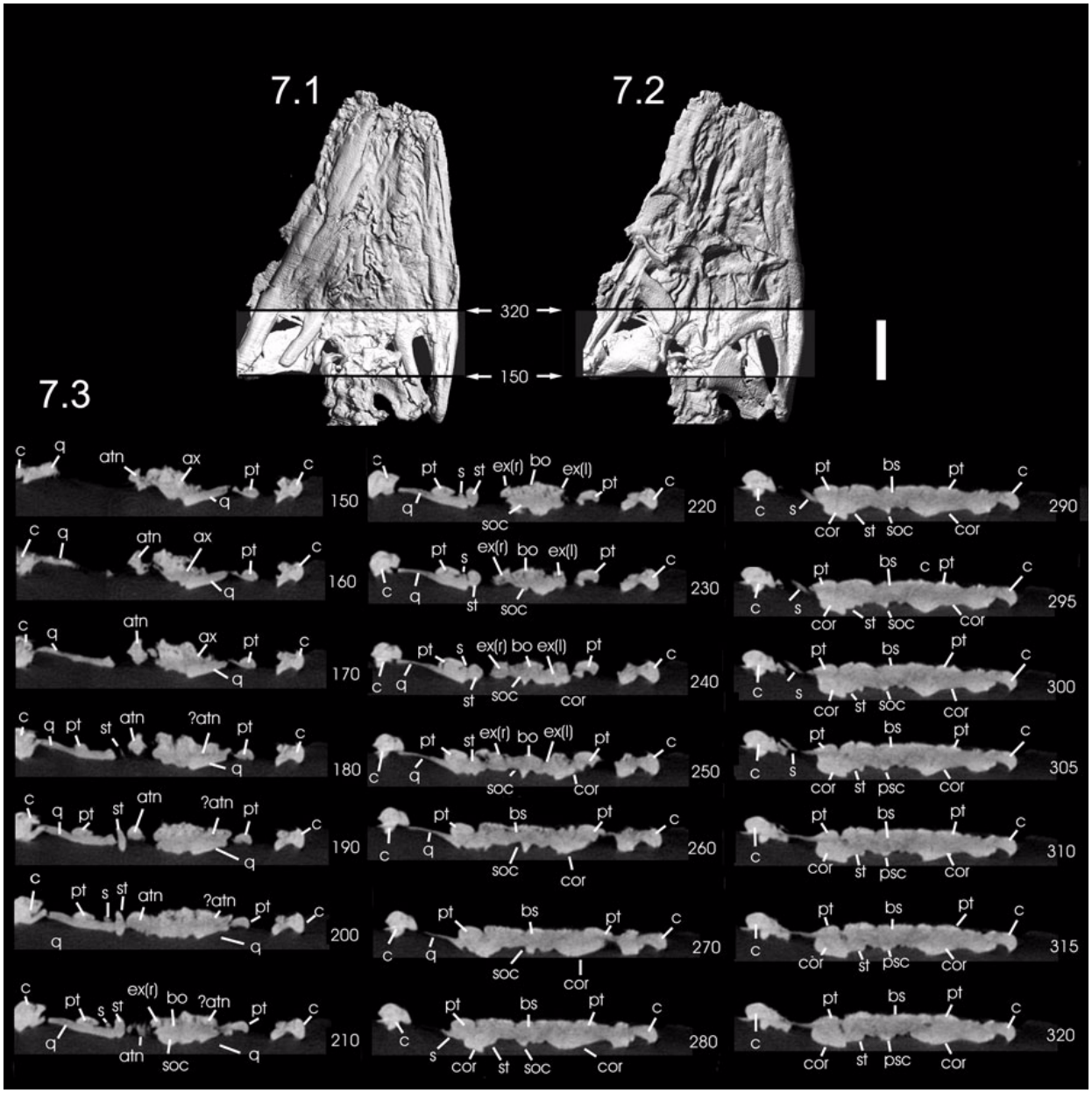

Figure 7. Computer generated views of the skull of *Pachyrhachis problematicus* specimen (HUJ-PAL 3659) in (7.1) ventral and (7.2) dorsal views; 7.3, serial sections of the area indicated by highlighted section of surface model, representing every tenth slice from 150 through 320 to illustrate the topological relationships of elements in the posterior portion of the skull. Abbreviations: atn, atlas neural arch; ax, axis vertebra; bs, basisphenoid; bo, basioccipital; c, compound bone; cor, coronoid; ex, exoccipital; psc, parietal sagittal crest; pt, pterygoid; q, quadrate; s, stapes; so, supraoccipital; st, supratemporal. Scale bar equals one centimeter.

The main body of each dentary is preserved nearly perpendicular to its anatomical position causing the anterior medial portion to deform, twisting nearly 90 degrees, resulting in an area of crushing and fractures that can be seen in serial section (Figure 8.2-8.7). One of the foramina (Figure 8.1, arrow 2) can be traced into unfractured bone, has well-defined edges, and is interpreted here as a single and only true mental foramen. A single mental foramen is characteristic of Serpentes (Rieppel et al. 2003; Lee and Caldwell 1998).

Circumorbital Series

All authors agree on the identification of the postorbitals lying symmetrically on either side of the skull. Medial extensions (Figure 5, ue4 and ue5) of the postorbitals, overlying the anterior parietal as illustrated by Caldwell and Lee (1997), gives them a lizard-like appearance (Figure 2.2).

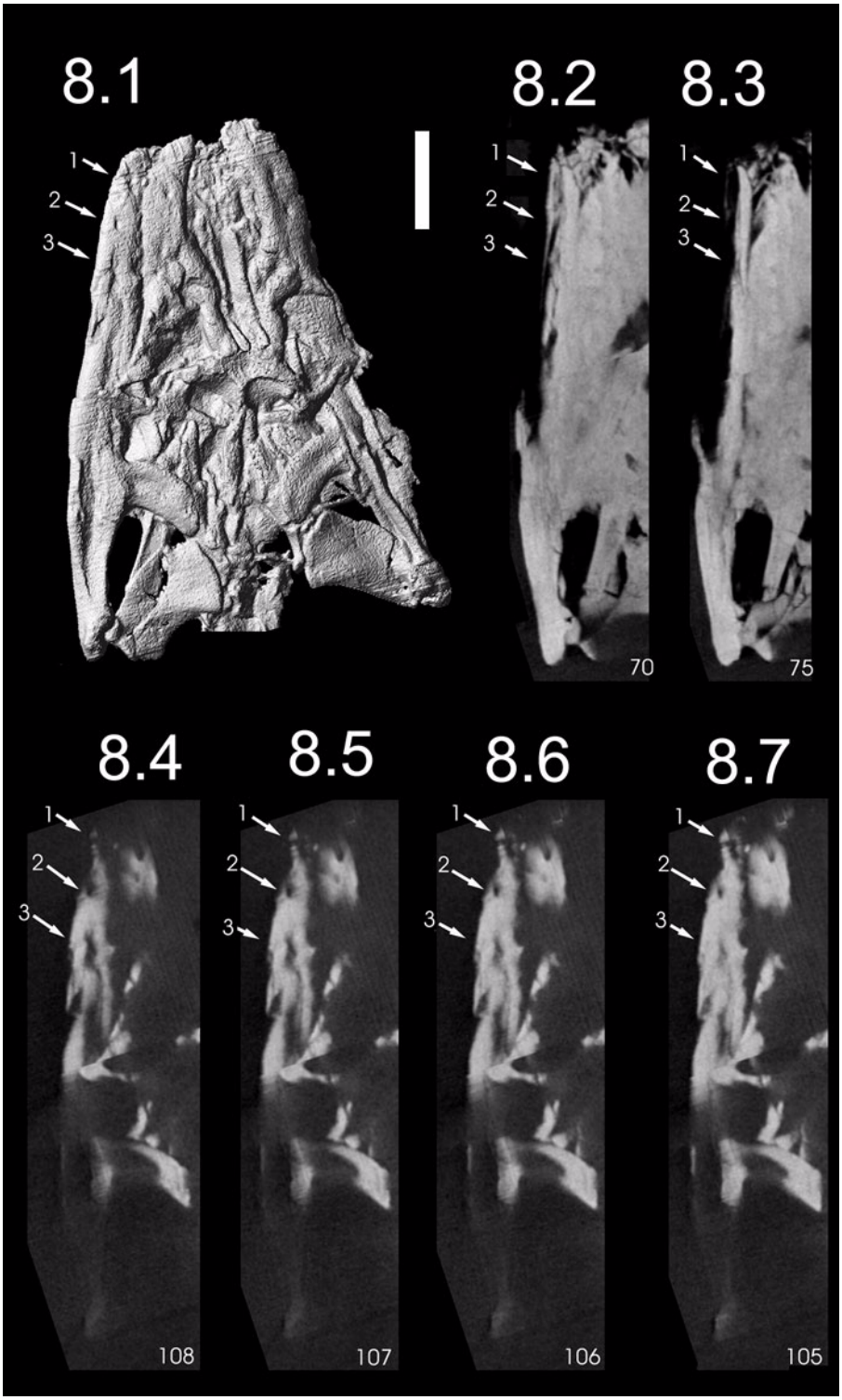

Figure 8. Skull of *Pachyrhachis problematicus* (HUJ-PAL 3659) in dorsal view and serial sections, illustrating mental foramen path and crushed regions. 8.1, dorsal view, computer generated reconstruction. Arrow 3 indicates depression identified by Caldwell and Lee (1997) as a second mental foramen. Arrow 1 indicates similar crushed region superficially resembling mental foramen; arrow 2 points to true mental foramen. 8.2 and 8.3, serial sections illustrating the relationship of the anterior crushed region, manifested in the superficial anterior depression in 8.1, arrow 1; 8.4-8.7, sequential serial sections demonstrating the relationship of external morphology to internal crushed regions. In serial section 8.7, the foramen indicated by arrow 2 can be traced through the sections without interruption; however, the superficial depressions mimicking foramina directly overlay crushed regions. Arrow 3 overlies the area weakened by the void of the Meckel's groove below and the anterior surangular suture above, and arrow 1 overlies the anterior crushed region formed by coronal rotation of the anterior dentaries. Scale bar equals one centimeter.

However, Zaher and Rieppel (1999) did not figure the medial structure as part of the postorbital but did indicate topographical relief in their interpretive drawing on the left side of the skull (Figure 2.3). It is unclear from the isosurface reconstruction (Figure 5.4, 5.5; see also Appendix 2) if the medial extensions were ever in contact with the undisputed portion of the postorbitals. However, it is clear that they are now topologically displaced and discontinuous with the postorbitals. The structures lie in a portion of the parietal table that is crushed and distorted. The structures themselves may be artifacts caused by crushing on top of the basipterygoid processes (Figure 5.4, 5.5). In any event the identity of these structures is ambiguous at best.

The most controversial elements in the skull of *Pachyrhachis* are those variably referred to as postfrontals by Haas (1979), as jugals by Caldwell and Lee (1997), and the broken anterior ectopterygoids by Zaher and Rieppel (1999). They are shown here in Figure 5.5 (elements labeled ue1 and ue2). These elements are in close proximity to the distal terminus of the undisputed postorbitals lying somewhat symmetrically on the suborbital process of the maxillae. We are reticent about precisely identifying ue1 and ue2 as postfrontals, ectopterygoids, or jugals, because the evidence for each is the same, namely where they lie.

No recent author agrees with Haas's (1979) identification of these elements as postfrontals. Given that the apparent force vector responsible for the crushing was dorsoventral, it is unlikely that the postfrontals would settle in the oblique position of these bones.

Supporting the argument of Zaher and Rieppel (1999b) that ue2 is a broken fragment of an ectopterygoid, is the fact that the right dentary is rotated under the skull, interrupting the natural position of the right ectopterygoid relative to the maxilla and pterygoid (Figure 5.1-5.5) and potentially causing breakage. The right pterygoid is displaced anteriorly and rotated to overlap slightly the parasphenoid (Figure 5.3). Thus it could have applied anteriorly directed force to the ectopterygoid and possibly caused breakage and displacement. Given the foreshortening of the left side of the skull and the leftward rotation of the snout, the ectopterygoid could have compressed in its long axis, retaining its natural anterior articulation with the maxilla, the broken posterior portion rotating clockwise and medially, coming to rest in its current position.

Arguing against identification as an ectopterygoid is Haas's (1979) correct (in our opinion) identification of the ectopterygoid on the left side and the otherwise consistent symmetry of other elements of the skull. Element ue3 lies medial to the dentary and is identified here as anterior right ectopterygoid (Figure 5.5; see also Appendix 2 and 3 for illustration of topological and dorsoventral relationships). Additionally, element ue1 on the left side and ue2 on the right are more or less symmetrically displaced (Figure 5.4 and 5.5). However, the left mandible could not have applied the same amount and direction of force on the left ectopterygoid as on the right, because the left mandible now lies lateral to and does not interfere with the natural position of the left ectopterygoid. It is also unlikely that sufficient force could be applied to the ectopterygoids to cause the pattern of breakage and displacement preserved in ue1 and ue2. We reject the hypothesis that the elements are displaced broken ectopterygoids on the basis of identification of the intact ectopterygoids and taphonomic interpretations.

Caldwell and Lee's (1997) identification of the elements ue1 and ue2 as jugals is topologically plausible in part. However, their interpretation presents three issues. First, there is no clear and definitive justification for the presence of a jugal except topological position in relation to the maxillae, but, given the taphonomic affects identified herein, that same evidence is applicable and equally compelling with respect to the other alternatives. Second, the element's relationship to the postorbitals and maxillae as preserved is problematic as there is no clear articulation facet or suture with either element (Appendix 3). Additionally, the position of the right and left elements relative to the maxillae are different. The medial portion of the left element is in contact with the maxilla whereas the lateral portion of the right element overlies the maxilla. Therefore, other than proximity to the postorbitals, there is no clear indication of articulation with the maxillae. Third, the morphology of the element is inconsistent with the morphology of the jugal in any known squamate in that it is merely a flat piece of bone that widens anteriorly and thus displays no morphology that clearly defines it as a jugal. Jugals have been reported as present in *Dinylisia* (Estes et al. 1970), but their presence was subsequently contradicted by Caldwell and Albino (2002). Jugals are unknown in all other snakes. We reject the hypothesis that *Pachyrhachis* had jugals on the basis of its morphology, topological relationships, and taphonomic considerations.

The identity of the elements ue1 and ue2 is most parsimoniously explained as the ventral portion of elongate postorbitals. The undisputed postorbitals are in fact the dorsal portion of the postorbitals and share a long articulation with the

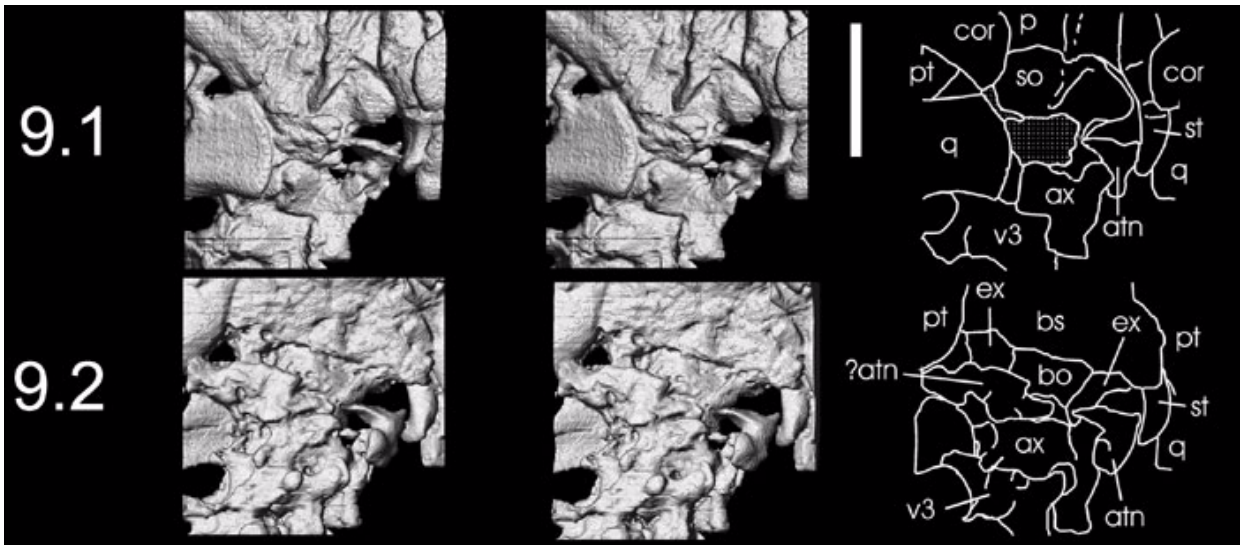

Figure 9. Stereopairs and line drawings of posterior portion of skull of *Pachyrhachis problematicus* (HUJ-PAL 3659), from computer reconstructed surface model derived from CT data in (9.1) dorsal and (9.2) ventral views. Abbreviations: atn, atlas neural arch; ax, axis vertebra; bs, basisphenoid; bo, basioccipital; cor, coronoid; ex, exoccipital; p, parietal; pt, pterygoid; q, quadrate; s, stapes; so, supraoccipital; st, supratemporal; V3, 3rd cervical vertebra.

anterolateral parietal, and likely contacted the frontal as in some macrostomatans (Lee and Scanlon 2002b, figure 2 d,e,f). This is supported by multiple lines of evidence: 1) the anterior portions of both of the ectopterygoids are visible in dorsal view; 2) the ventral ends of both ue1 and ue2 are in contact with the anterior ends of the ectopterygoids; 3) the dorsal ends are in contact with the undisputed postorbitals; 4) the combined length of the undisputed portion of the postorbitals and their ventral counterparts is accommodated by the anterolaterally elongate parietal; and 5) taphonomic affects evidenced in the distortion of other morphology suggest predominantly dorsoventral forces acted upon the fossil and thus would reasonably produce the resultant configuration of the postorbitals, ue1, and ue2. Figure 4 illustrates the effects of crushing on HUJ-PAL 3659 (See also Appendix 4 for animation sequence of crushing).

Exoccipitals

The exoccipitals are compact and project only a short lateral distance (Figure 9.2). The area above the basioccipital preserves the supraoccipital but obscures the foramen magnum (Figure 9.1). There is evidence of' slight crushing parasagittally on the dorsal surface of the supraoccipital, indicating weak support from below and allowing the possibility of separation of the exoccipitals. However, this character remains inconclusive and must be treated as unknown in *Pachyrhachis*. Exclusion of the supraoccipital from the foramen magnum by contact of the exoccipitals has long been considered a synapymorphy of Serpentes (Underwood 1967; Rieppel 1979; Estes et al. 1988), but Zaher and Rieppel (2002) indicate this character appears to be variable within Macrostomata.

Dorsal Laminae of Maxillae

Haas (1979) mistook the left prefrontal for the frontal. Caldwell and Lee (1997) correctly identified prefrontals and frontals but reconstruct an ascending process of the maxillae, overlapping the prefrontal. Zaher and Rieppel (1999b) illustrate the structure as a portion of the prefrontal. The area in question is separated from the maxillae on both the right and left sides and is displaced ventrally relative to the preserved dorsal surface of the maxillae. Light photographs demonstrate artifacts of shadow and surface irregularity that obfuscate morphology when compared with surfaces derived from CT data as evidenced in Appendix 2. Comparing the light photographs and the CT renderings, it is clear these bones are separate from both the maxillae and the prefrontals, albeit not in a uniform way. The narial margin in *Pachyrhachis* can be traced up to and including the prefrontals, but unambiguous delineation of where the prefrontals end and the maxillae begin is difficult. However, the more posterior portion of the external nares curve medially as preserved and thus would indicate at least a moderate development of the dorsal laminae of the maxillae and that interpretation is accepted here. Some alethinophidians retain a modest dorsal lamina of the maxilla at the point of articulation with the prefrontal as in *Cylindrophis* (Lee and Caldwell 2002, figure 4B). The presence of dorsal laminae

Table 1. Comparison of interpretation of selected morphology from previous and current studies of *Pachyrhachis problematicus.* Ue1-ue5 refer to the elements illustrated in figure 5 of this study. See Figure 2 for illustrations and interpretations of previous studies.

Haas 1979, 1980a	Caldwell and Lee 1997	Zaher and Rieppel, 1999b	This Study
Postfrontals	Jugals	Broken displaced anterior ectopterygoids	Ventral portion of postorbitals (ue1&ue2)
Not applicable	Postfrontal fused to postorbital	Crushed frontalis decensus	Anterior portion of ectopterygoid (ue3)
Anterior portion of left ectopterygoid	Posterior left maxilla	Not applicable	Anterior portion of left ectopterygoid
Posterior portion of left ectopterygoid	Ectopterygoid	Not applicable	Posterior portion of left ectopterygoid
Right ectopterygoid	Posterior right maxilla	Posterior right maxilla	Posterior right maxilla
Not applicable	Medial processes of postorbital	Not part of postorbital	Possibly crushing of parietal table (ue4&ue5)
Stapes	Tentative squamosal	Stapes	Stapes
Not applicable	Stapes	Paroccipital process of opisthotic	Stapes
Not applicable	Vertically oriented quadrate	Posterventrally inclined quadrate	Posteroventrally inclined quadrate
Not applicable	Two mental formina	One mental foramen	One mental foramen
Not applicable	Broad lateral profile of quadrate	No suprastapedial process of quadrate	No suprastapedial process of quadrate
Not applicable	Broad lateral profile of quadrate	More Macrostomatan-like quadrate	Stylohyal process on ventral medial margin
Not applicable	Exoccipitals do not contact	Unknown	Unknown

does not exclude interpretation of *Pachyrhachis* at least at the level of Alethinophia.

Summary of Characters

Of the six characters examined all have been shown to: 1) have been misinterpreted; 2) possess the Serpentes, the alethinophidian, or the macrostomatan condition; or 3) be absent or ambiguous. Table 1 summarizes the interpretations of this study in comparison to previous studies. The quadrate lacks a suprastapedial process. A stylohyal process is present on the ventral medial shaft. The posteriorly projecting supratemporal provides sole support for the quadrate, which is inclined. *Pachyrhachis* is shown to possess an elongate and slender stapes and a single mental foramen. A jugal is absent, and the elements referred to herein as ue1 and ue2 are considered the ventral portion of the postorbital. The exoccipital contact above the foramen magnum is unknown. The maxillae possess a moderately developed ascending process.

The presence of a single mental foramen and loss of the jugal is diagnostic of Serpentes (Lee and Caldwell 1998; Tchernov et al. 2000). A dorsal lamina of the maxilla is present in alenthinophidians but is reduced in Recent macrostomatans. The dorsal laminae of *Pachyrhachis* are primitive. However, in Pachyrhachis the supratemporal provides sole support of the quadrate, the quadrate has a reduced suprastapedial process and a well-developed distomedial stylohyal process, and the stapes is long and slender. Thus, in respect to the quadrate suspensorium and morphology, *Pachyrhachis* displays the condition in macrotomatan snakes above the level of Loxemus and Xenopeltis (Tchernov et al. 2000). In the absence of characters eliminating *Pachyrhachis* from Serpentes and in the presence of skull characteristics otherwise diagnosing the macrostomatan condition as noted above, better support is found for the hypothesis placing Pachyrhachis problematicus as a basal macrostomatan (sensu Tchernov et al. 2000). Figure 10 illustrates our revised reconstruction of the skull of *Pahyrhachis problematicus*.

DISCUSSION AND CONCLUSIONS

Perhaps the most widely acknowledged character of snakes is the loss of limbs. However, only in derived macrostomatans is the loss of limbs total. Scolecophideans, pythons, and boas all retain vestiges of hind limbs or girdle elements. With the demonstration that *Pachyrhachis* and

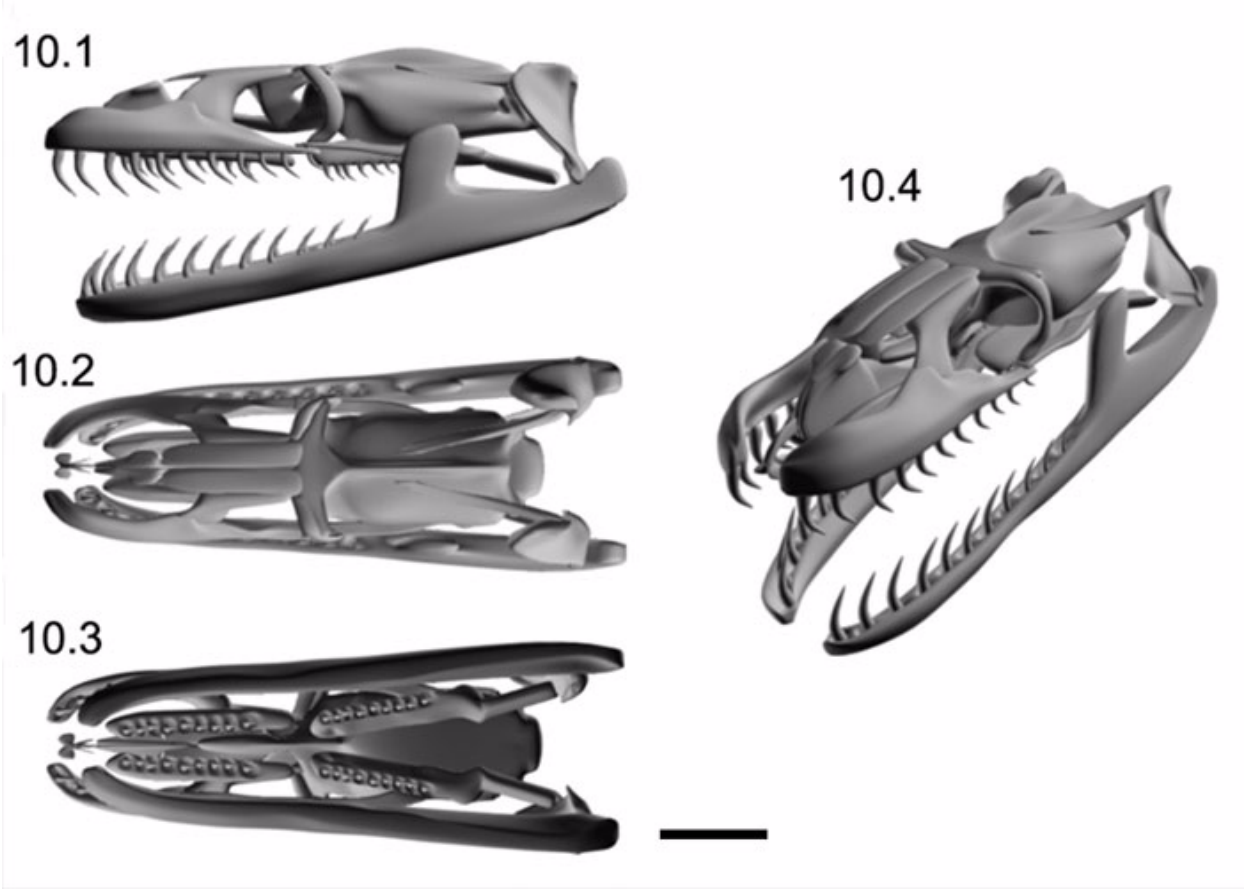

Figure 10. A-D. Morphological model of *Pachyrhachis problematicus* in (10.1) lateral view, (10.2) dorsal view, (10.3) ventral view, and (10.4) oblique view. This varies from Caldwell and Lee (1997) in the reconstruction and orientation of the quadrate, the ectopterygoid, and the circumorbital series. The nasals are conjectural as they are not preserved in the specimen. Discussion of the reconstruction of the quadrate and circumorbital bones is detailed in the text. Caldwell and Lee's (1997) reconstruction of the ectopterygoid is implausible as it would interfere with the natural position of the coronoid and not allow the jaws to be shut. Therefore, we reconstructed the ectopterygoids in a more medial position near the maxilla, allowing passage of the coronoid.

Haasiophis are macrostomatans (Tchernov et al. 2000), the occurrence of hind limbs with a complete bony complement attains added significance. Although Tchernov et al. (2000; see also Zaher and Rieppel 1999) entertained the possibility (on the basis of parsimony analysis) that legs may have re-evolved in macrostomatans, that possibility now seems remote. In and of itself, the loss and re-attainment of a complex element or character within a specific monophyletic group is always less parsimonious than a single loss. The interpretation of limb reacquisition as more parsimonious is possible only in the context of tree topology based on other characters not related to the one in question, and on the acceptance of reduced limbs as a basal synapomorphy within Serpentes.

Tree topology is accepted on the basis of parsimony. Character interpretation as homoplasy, synapomorphy, or symplesiomorphy is guided by the test of congruence. But neither parsimony analysis nor interpretations of characters based on tests of congruence are explicitly accompanied by an understanding of genetic, developmental, or other biological processes involved with the loss or gain of a character. Therefore, analysis and interpretation of character distribution should, when possible, be performed in the context of an understanding of biological processes rooted in empirical evidence and experimentation.

Independent of limb development, the morphological interpretation of the skull presented here is consistent with a phylogenetic placement of *Pachyrhachis* as a basal macrostomatan. Retention of limbs in a relatively advanced snake has implications for the developmental model of limblessness and axial patterning as presented by Cohn and Tickle (1999) who studied the genetic control and developmental process of limb loss in snakes. Their model accepted *Pachyrhachis* as the sister taxon to Serpentes and thus favored loss of

distal limb elements in basal Serpentes, and total loss in advanced snakes. In that study, fibroblast growth factors were grafted to *Python* limb buds and successfully stimulated outgrowth. They were unable to stimulate apical ridge development, but did demonstrate polarizing potential by grafting the *Python* limb buds to the wing area of mutant wingless chicken embryos. The development of limbs in treated wingless chicken embryos demonstrated that *Python* hind limb mesenchyme conserves coding for limb development and polarization, and that suppression of limb development in *Python* is due to absence of apical ridge development.

Hind limbs occasionally occur in whales as in the humpback whale specimen documented by Andrews (1921) that possessed a cartilaginous femur, osseous tibia, cartilaginous tarsus, and osseous metatarsal. Reduction of hind limbs in whales is the result of arrested limb bud development (Bejder and Hall 2002). In humpback whales limb bud development persists longer than in odontocetes, partially explaining the more frequent expression in humpbacks. Presumably the loss of hind limbs in whales is accomplished by similar developmental and genetic processes as in other limbless vertebrates. However, the occasional occurrence of hind limbs in whales is a variant within a species and is quantitatively different from the fixed presence of hind limbs implicit in *Pachyrhachis* and *Haasiophis*. The variable presence of hind limbs in whales speaks to the process of limb loss, and does not necessarily speak to the genetic or developmental processes of reacquisition unless the assumption is made that the processes and controls elucidated by Cohn and Tickle (1999) are easily reversed. There is no direct supporting evidence to suggest that reacquisition of limbs after loss has ever occurred.

In insects, the reacquisition of wings has recently been hypothesized (Whiting et al. 2003). That study, based on molecular phylogenetic analysis, suggested the reacquisition (versus multiple loss of wings) based on parsimony analysis, similar to the situation we face with limb presence in basal macrostomatans. However, the conclusion that wings re-evolved after loss is again based on the parsimony analysis and tests of congruence of character distribution, a distribution that may have nothing to do with the genetic control, development, or other fundamental biological attributes of wings. In that case, one could reasonably predict that with further acquisition and analysis of character data, the hypothesis of re-evolution of insect wings will be falsified.

Clearly, expansion of the thoracic identity in the axial skeleton, most likely controlled by Hox gene expression domains, is an early development in snake evolution. Additionally, Hox gene expression related to apical ridge development in hind limb buds may control further limb loss. The recognition of the derived nature of *Pachyrhachis* demonstrates that leg loss under such a model is more variable in snakes than recognized previously because the hind limb skeleton of *Pachyrhachis* is better developed than in either boas and pythons or worm snakes (scolecophideans). However, this variation merely implies that hind limb loss in snakes is more complicated than a progressive decrease in development through time, and that hind limbs were reduced separately in more than one clade. This also appears to be the case in a recent study of limblessness in anguid lizards (Wiens ands Slingluff 2001). Given the hypothesis that snakes are evolved from within Squamata, retention of hind limbs, a plesiomorphic structure in tetrapods, is not surprising nor is it informative in a cladistic sense.

The interpretation of limb retention in *Pachyrhachis* and related forms implies multiple limb reductions in scolecophidians, alethinophidians, and within macrostomatans. This scenario appears likely given our current understanding of developmental mechanisms controlling limb expression, does not require an additional *ad hoc* hypothesis of biological processes controlling redevelopment, and is therefore a more parsimonious conclusion compared to reacquisition. The total elimination of hind limb specification and its skeletal remnants is characteristic of advanced macrostomatan snakes only.

Various interpretations of observed morphology placed *Pachyrhachis* in a more primitive and basal position among snakes, or in a derived phylogenetic position as a macrostomatan. Computed tomography allows a more thorough examination of *Pachyrhachis problematicus* than previously available and therefore provides for revised reconstruction and modeling of the skull, especially with respect to the morphology and position of the quadrates, the identity of the circumorbital bones, and the identity and position of the ectopterygoid. There is no compelling evidence for retention of a squamosal, a jugal, vertical orientation of the quadrate, or retention of multiple mental foramina. This analysis confirms the presence of a posterior free-ending projection of the supratemporals with distal expansion providing sole support of the quadrates, quadrate with no suprastpedial process but with a stylohyal process. The contact of the exoccipitals above the foramen magnum is ambiguous. Our analysis favors the phylogentic hypothesis that *Pachyrhachis* is a basal macrostomatan, consis-

tent with the conclusions of Zaher (1998; see also Zaher and Rieppel 1999b; Tchernov et al. 2000).

ACKNOWLEDGMENTS

We would like first to acknowledge Will Downs, to whose memory we dedicate this work. Will had a quick and creative mind and was always anxious to look at interesting fossils in ways that shed new light. Thanks to R. Ketchum of the University of Texas at Austin High Resolution CT facility for scanning services and advice. Thanks to K. Newman, D. Winkler, and D. Vineyard for assistance in many aspects of this project. C. Bell provided access to comparative specimens. We thank G. Bell for useful comments and discussion of earlier versions of this work. Thanks to O. Rieppel and M. Caldwell for thorough and constructive reviews of this paper. This project was supported by the National Geographic Society and the Institute for the Study of Earth and Man at Southern Methodist University. Finally we would like to remember Eitan Tchernov. We will miss his friendship and enthusiasm for our joint studies of the fossils of 'Ein Yabrud.

REFERENCES

Adobe Systems Inc. 2001. *Adobe Photoshop version 6.0.1*. Adobe Systems Incorporated, San Jose, California,USA.

Andrews, R.C. 1921. A remarkable case of external hind limbs in a humpback whale. *American Museum Novitates*, 9:1–6.

Bejder, L. and Hall, B.K. 2002. Limbs in whales and limblessness in other vertebrates: mechanisms of evolutionary and developmental transformation and loss. *Evolution & Development*, 4:445–458.

Caldwell, M.W. 1999. Squamate phylogeny and the relationships of snakes and mosasauroids. *Zoological Journal of the Linnean Society*, 125:115–147.

Caldwell, M.W. 2000. On the phylogenetic relationships of *Pachyrhachis* within snakes: a response to Zaher (1998). *Journal of Vertebrate Paleontology*, 20:187–190.

Caldwell, M.W. and Lee, M.S.Y. 1997. A snake with legs from the marine Cretaceous of the Middle East. *Nature*, 386:705–709.

Caldwell, M.W. and Albino, A. 2002. Exceptionally preserved skeletons of the Cretaceous snake *Dinilysia patagonica* Woodward, 1901. *Journal of Vertebrate Paleontology*, 22:861–866.

Cohn, M.J. and Tickle, C. 1999. Developmental basis of limblessness and axial patterning in snakes. *Nature*, 399:474–479.

Cope, E.D. 1869. On the reptilian orders Pythonomorpha and Streptosauria. *Proceedings of the Boston Society of Natural History*, 12:250–266.

Estes, R., Frazzetta, T.H. and Williams, E.E. 1970. Studies on the fossil snake *Dinilysia patagonica* Woodward. Part I. Cranial morphology. *Bulletin of the Museum of Comparative Zoology*, 140:25–74.

Estes, R., de Queiroz, K., and Gauthier, J. 1988. Phylogenetic relationships within Squamata. In Estes, R. and Pregill, G. (eds), *Phylogenetic Relationships of the Lizard Families: Essays commemorating Charles L. Camp*. Stanford University Press: Stanford, California, pp. 119-270.

Haas, G. 1979. On a new snakelike reptile from the Lower Cenomanian of Ein Jabrud, near Jerusalem. *Bulletin du Muséum national d'Histoire naturelle, Paris (Series 4)*, 1:51–64.

Haas, G. 1980a. *Pachyrhachis problematicus* Haas, snakelike reptile from the Lower Cenomanian: ventral view of the skull. *Bulletin du Muséum national d'Histoire naturelle, Paris (Series 4)*, 2:87–104.

Haas, G. 1980b. Remarks on a new ophiomorph reptile from the lower Cenomanian of Ein Jabrud, Israel, p. 177–192. In Jacobs, L.L. (ed.), *Aspects of Vertebrate History*, Museum of Northern Arizona Press, Flagstaff, Arizona.

Lee, M.S.Y. 1997a. On snake-like dentition in mosasaurian lizards. *Journal of Natural History,* 31: 303-314.

Lee, M.S.Y. 1997b. The phylogeny of varanoid lizards and the affinities of snakes. *Philosophical Transactions of the Royal Society of London B* 352: 53-91.

Lee, M.S.Y. and Caldwell, M.W. 1998. Anatomy and relationships of *Pachyrhachis problematicus*, a primitive snake with hindlimbs. *Philosophical Transactions of the Royal Society of London B*, 352:1521–1552.

Lee, M.S.Y. and Scanlon, J.D. 2002a. The Cretaceous marine squamate *Mesoleptos* and the origin of snakes. *Bulletin of the Museum of Natural History, London,* 68(2):131–142.

Lee, M.S.Y. and Scanlon, J.D. 2002b. Snake phylogeny based on osteology, soft anatomy and ecology. *Biological Reviews*. 77:333–401.

Newtek Inc. 2004. Lightwave 3D. Newtek Incorporated. San Antonio, Texas.

Rage, J.C. and Escuillie´, F. 2000. Un nouveau serpent bipède du Cénomanien (Crétacé). Implications phylétiques. *Comptes Rendus de l'Académie des Sciences de Paris, Sciences de la Terre et des Planètes*, 330:513–520.

Rasband, W. 2003. ImageJ version 1.31. *National Institutes of Health*. Bethesda, Maryland, USA.

Rieppel, O. and Kearney, M. 2001. The origin of snakes: limits of a scientific debate. *Biologist*. 48:100–114.

Rieppel, O. 1979. A cladistic classification of primitive snakes based on skull structure. *Z. Zool. Syst. Evolutionsforsch.* 17:140-150.

Rieppel, O. and Zaher, H. 2000a. The intramandibular joint in squamates, and the phylogenetic relationships of the fossil snake *Pachyrhachis problematicus* Haas. *Fieldiana, Geology*, 43:1–69.

Rieppel, O. and Zaher, H. 2000b. The braincases of mosasaurs and *Varanus*, and the relationships of snakes. *Zoological Journal of the Linnean Society*, 129:489–514.

Rieppel, O., Zaher, H., Tchernov, E., and Polcyn, M.J. 2003. The anatomy and relationships of *Haasiophis terrasanctus*, a fossil snake with well-developed hind limbs from the mid-Cretaceous of the Middle East. *Journal of Paleontology*, 77(3):536–558.

Tchernov, E., Rieppel, O., Zaher, H., Polcyn, M.J., and Jacobs, L.L. 2000. A fossil snake with limbs. *Science*, 287:2010–2012.

Underwood, G. 1967. A contribution to the classification of snakes. *British Museum* (*Natural History),* 653:1–179.

Vaytek, 2000. Voxblast 3.0. *Image Analysis Facility*. University of Iowa, Ames, Iowa, USA.

Whiting, M.F., Bradler, S., and Maxwell, T. 2003. Loss and recovery of wings in stick insects. *Nature*, 421:264–267.

Wiens, J.J. and Slingluff, J.L. 2001. How lizards turn into snakes: A phylogenetic analysis of body-form evolution in anguid lizards. *Evolution,* 55(11):2303–2318.

Zaher, H. 1998. The phylogenetic position of *Pachyrhachis* within snakes (Squamata, Lepidosauria). *Journal of Vertebrate Paleontology*, 18:1–3.

Zaher H, and Rieppel O. 1999a. Tooth implantation and replacement in squamates, with special reference to mosasaur lizards and snakes. *American Museum Novitates* 3271: 1-19.

Zaher, H. and Rieppel, O. 1999b. The phylogenetic relationships of *Pachyrhachis problematicus*, and the evolution of limblessness in snakes (Lepidosauria, Squamata). *Comptes Rendus de l´Académie des Sciences de Paris, Sciences de la Terre et des Planètes*, 329:831–837.

Zaher, H. and Rieppel, O. 2000. A brief history of snakes. *Herpetological Review*, 31:73–76.

Zaher, H. and Rieppel, O. 2002. On the phylogenetic relationships of the Cretaceous snakes with legs, with special reference to Pachyrhachis problematicus (Squamata, Serpentes) *Journal of Vertebrate Paleontology,* 2002, 22(1):104-109

Appendix 1. CT data set of *Pachyrhachis problematicus* (HUJ-PAL 3659). **1.1,** Original data set; **1.2,** data set aligned and resampled in the XZ axis.

1.1

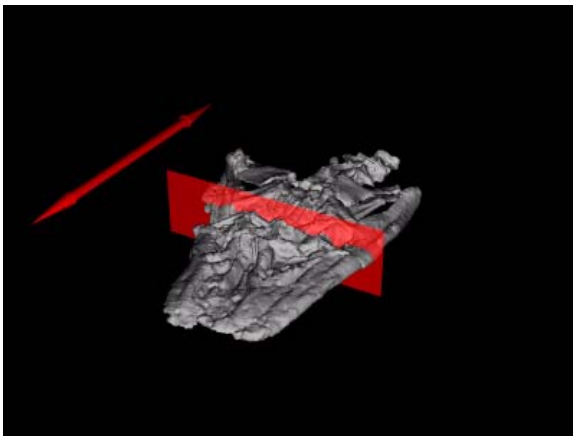

1.2

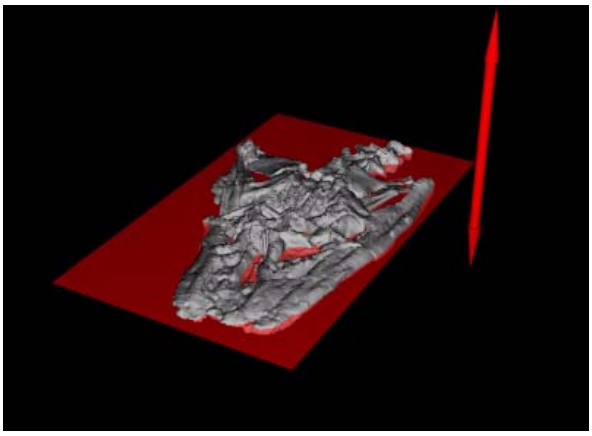

Appendix 2. Comparison of light photograph of the anterior dorsal portion of *Pachyrhachis problematicus* (HUJ-PAL 3659) and CT reconstruction of densities represented as a surface model. Note artifacts introduced by lighting conditions and differences in apparent surface fractures, morphology, and sutures when comparing the light photograph and the density derived model. For example, crushing into the Meckel's groove previously interpreted as a second mental foramen, morphology of purported medial process of postorbital, the relationship of the maxillae to the prefrontals, and the posterior margin of the parietal table.

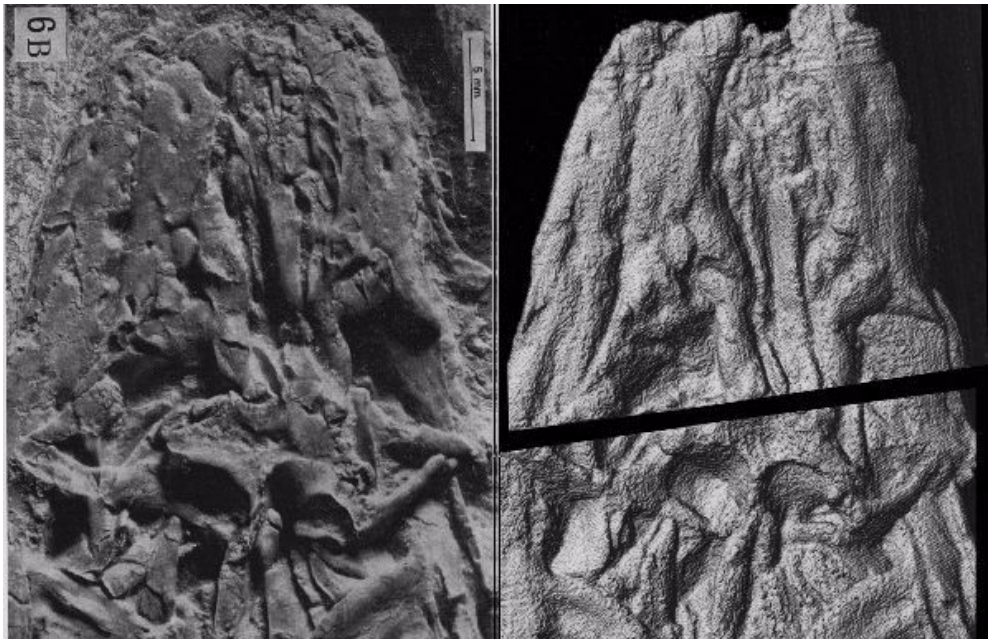

Appendix 3. Comparison of dorsal and ventral CT reconstructions illustrating alignment of dorsal and ventral structures. Note the position of ventral portion of the postorbitals (ue1 and ue2 in Figure 5) in relation to the anterior portion of the ectopterygoids (left ectopterygoid and ue3 in Figure 5).

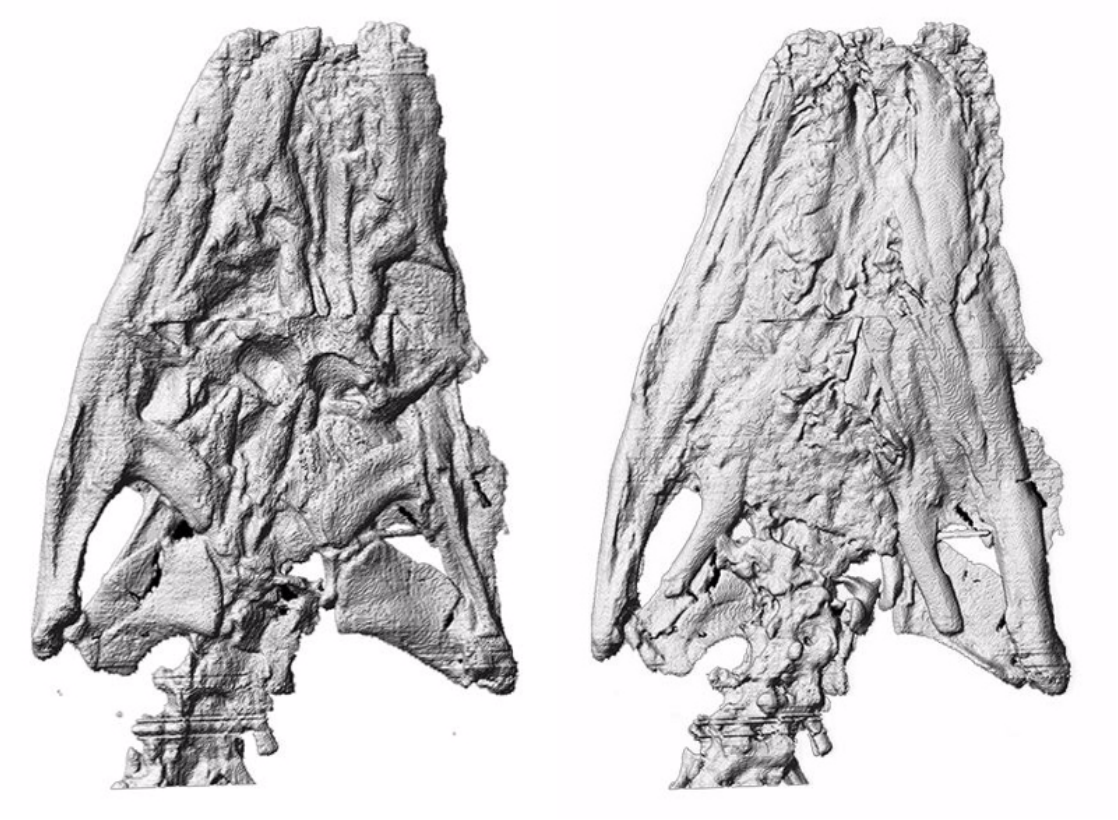

Appendix 4. Animation sequence illustrating taphonomic affects on the preservation of *Pachyrhachis problematicus* (HUJ-PAL 3659).

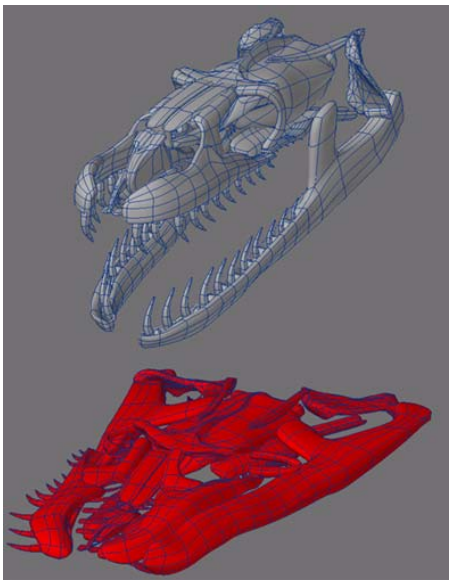

Appendix 5. Digital reconstruction of the quadrate of *Pachyrhachis problematicus.* Animation sequence showing extraction of region of interest, rotation of region of interest, removal of elements other than quadrate, removal of crushing of the quadrate, and rotation of restored quadrate. Removal of crushing was accomplished by alignment of the cephalic condyle long axis with the sagittal axis of the skull and alignment of the mandibular condyle orthogonal to the manidibular long axis. A crack apparently due to extensional forces was eliminated by a slight anterior rotation of the distal portion of the quadrate. Note the lack of suprastapedial process and the presence of a stylohyal process on the distal medial shaft.